

**Blast and Fire Resistant Material****B A M****EXCELLENCE/0421/0137****DELIVERABLE D4.2****VALIDATION OF MATERIALS IN THE LABORATORY**

## Project Information

Project Title	Blast and Fire Resistant Material
Project Acronym	BAM
Programme	EXCELLENCE HUBS
Grant Number	EXCELLENCE/0421/0137
Project Duration	01.04.2022 – 31.03.2024 (24 months) + 3 months extension

## Document information

Deliverable Number	D4.2
Deliverable Title	Validation of Materials in the Laboratory
Version	1.0
Dissemination Level	Public
Work package	WP4
Authors	Ioanna Giannopoulou (FRC), Thomaïda Polydorou (UCY), Andreas Lampropoulos (UBrighton)
Contributing partners	FRC, UCY, UBrighton
Delivery Date	28.06.2024
Planned Delivery Month	M22
Keywords	Materials, Validation, Testing, Fire, Impact, Laboratory

## Version History

No	Description	Author	Organization	Date
1	First draft	Dr Ioanna Giannopoulou Dr Thomaïda Polydorou	FRC UCY	21.03.2024
2	Second draft with the addition of Partners' contribution	Dr Ioanna Giannopoulou	FRC	15.05.2024
3	Review of the document	Dr Demetris Nicolaides Prof Michael Petrou Dr Andreas Lampropoulos Dr Ourania Tsioulou	FRC UCY UBrighton UBrighton	03.06.2024
4	Final version with integration of the reviewers' feedback	Dr Ioanna Giannopoulou	FRC	28.06.2024

## Table of Contents

EXECUTIVE SUMMARY .....	5
LIST OF FIGURES .....	6
LIST OF TABLES.....	7
1. Introduction.....	8
2. Validation of the impact- and blast-resistant material performance .....	9
3. Validation of the Fire-Resistant Geopolymers Performance .....	19
3.1 The Fire-Resistant Geopolymer (FRG) layer of the HLM.....	19
3.2 The Smart Composite Geopolymeric Concrete (SCGC) .....	22
4. Comparative Analysis of Fire Resistance in Standard Concrete and the New Materials HLM and SCGC .....	25
4.1 Materials and methods .....	25
4.2 Fire Exposure Testing .....	28
4.3 Data Collection .....	29
4.4 Data Visualization.....	30
4.5 Data Analysis .....	31
5. Conclusions.....	36
<b>Acknowledgements .....</b>	<b>38</b>

## EXECUTIVE SUMMARY

The key objective of the research project “***Blast and Fire Resistant Materials (BAM)***” was the design and development of innovative, sustainable, and low cost construction materials, with combined blast/impact- and fire-resistance. These materials were aimed to be capable of dispersing the energy of blast/impact loads by enhancing their ductility and toughness and simultaneously, protecting the structure from a fire incident that may follow or proceed. Specifically, BAM research project deals with the design and development of (i) a Hybrid Laminated Material (HLM) in WP3, Task 3.1, which consists of an Ultra-High Performance Fibre Reinforced Concrete (UHPFRC) with blast and impact resistance and a superficial layer of a fire resistant geopolymer (FRG) and (ii) a Smart Composite Geopolymer Concrete (SCGC) in WP3, Task 3.2, which has dual functionality, i.e., of fire and blast/impact resistance.

Deliverable “***D4.2-Validation of Materials in Laboratory***” presents the results of the laboratory scale assessment of both developed materials (i.e., HLM and SCGC) properties. The most important process parameters affecting the targeted properties of materials were identified and investigated, to optimize the materials performance against blast, impact and fire. Among the investigated parameters, the water-to-binder ratio for the UHPFRC and the rheology for the FRG and SCGC were considered the most significant. The targeted properties of the UHPFRC layer of the HLM included high compressive and flexural strengths, and resistance against blast and impact, while those of the FRG layer included adequate mechanical strength, low density, fire resistance, thermal stability at elevated temperatures and structural integrity after exposure to fire. The SCGC material targets the combination of all the abovementioned properties, i.e. high compressive and flexural strengths, resistance against blast, impact and fire, low density, thermal stability at elevated temperatures and structural integrity after exposure to fire. The lab-scale validation of the SCGC material was carried out for both the production processes used: i.e., the conventional casting and the advanced 3D printing.

Both the new HLM and SCGC materials developed in the BAM project successfully met nearly all the targeted properties to a high standard.

## LIST OF FIGURES

<b>Figure 1:</b> Stress-strain relationship from loading cylindrical specimens in compression. ....	11
<b>Figure 2:</b> Stress-strain relationship from direct tension tests on dog-bone specimens. ....	11
<b>Figure 3:</b> Stress-strain relationship from direct tension tests on prismatic specimens. ....	11
<b>Figure 4:</b> (a) Dog-bone specimen (cross-sectional area 50 x 25mm) and (b) Prismatic specimen (cross-sectional area 100 x 50 mm). ....	12
<b>Figure 5:</b> Furnace temperature profile during the FRG material fire test (standard ISO 834 fire curve). ....	20
<b>Figure 6:</b> Temperature profile on the FRG specimen's front side, at a distance of 22 cm from the front side and at the interface of concrete slab. ....	21
<b>Figure 7:</b> The FRG specimen (a) before and (b) after the standard ISO 834 fire test. ....	21
<b>Figure 8:</b> Furnace temperature profile during the SCGC fire test (standard ISO 834 fire curve). ....	22
<b>Figure 9:</b> Temperature profile on the SCGC specimen's front side, at a distance of about 20 cm from the front side and at the interface of SCGC with the concrete slab. ....	23
<b>Figure 10:</b> The FRG specimen (a) before and (b) after the standard ISO 834 fire test. ....	23
<b>Figure 11:</b> Attachment of geopolymer layers to concrete cubes in HGFRL-CB [A] and SCGL-CB [B] systems. ....	27
<b>Figure 12:</b> Application of quartz adhesion primer [a] and sealant silicone [b] on the Surfaces of smart composite geopolymeric concrete and concrete cube. ....	27
<b>Figure 13:</b> Positioning of thermocouples in SCC, HGFRL-CC, and SCGM-CC systems during fire exposure. ....	28
<b>Figure 14:</b> Fire testing setup illustrating the placement of six thermocouples for monitoring temperature fluctuations inside concrete cubes. ....	28
<b>Figure 15:</b> PC interface connected to ESP32 board for recording temperature data from DS18B20 sensors. ....	29
<b>Figure 16:</b> Temperature variation over time for different concrete cubes configurations. ....	31
<b>Figure 17:</b> Exposed surface of (a) standard concrete cube (SCC) after fire testing; (b) of concrete cube with fire-resistant geopolymer layer (HGFRL-CC) after fire testing and (c) of concrete block with smart composite geopolymer layer (SCGL-CC) after fire testing. ....	34

## LIST OF TABLES

<b>Table 1:</b> Optimized mixture of UHPFRC. ....	10
<b>Table 2:</b> Optimized UHPFRC Material Properties.....	10
<b>Table 3:</b> Properties of the optimized FRG material.....	19
<b>Table 4:</b> Properties of the optimized SCGC material.....	22
<b>Table 5.</b> Mix design composition for standard concrete cubes (1 m <sup>3</sup> ). ....	25
<b>Table 6.</b> Mix design composition of hybrid laminate fire resistant geopolymer (900 cm <sup>3</sup> ). ....	26
<b>Table 7.</b> Mix design composition of smart composite geopolymer concrete (900 cm <sup>3</sup> ). ....	26
<b>Table 8.</b> Temperature data collected from thermocouples for standard concrete cube, hybrid geopolymer fire resistant layer, and smart composite geopolymer material during fire exposure. ....	30

## 1. Introduction

A key task planned in the frame of in the research project “**Blast and Fire Resistant Materials (BAM)**” was the design and development of a Hybrid Laminated Material, that consists of a blast- and impact-resistant layer of Ultra High Performance Fibre Reinforced Concrete (UHPFRC) and a fire-resistant layer of a geopolymer (FRG) material, based on industrial wastes and by-products. In addition, the project aimed at the design and development of a Smart Composite Geopolymer Concrete (SCGC) with combined blast-, impact- and fire-resistance. Deliverables “**D3.1- Design and Development of a Hybrid Laminated Material (HLM)**” and “**D3.2-Smart Composite Geopolymeric Concrete (SCGC)**” describe in detail the efforts performed for the design, development and optimization of both materials, i.e., the HLM and the SCGC. In Deliverable “**D4.1-Flowsheets of Materials Production**”, the detailed flow-diagrams of the procedures followed to produce these materials are presented, with both the investigating production methods, i.e., of conventional casting (HLM and SCGC) and advanced 3D printing (FRG, SCGC). Deliverable “**D4.2-Validation of Materials in the Laboratory**” presents the results of properties validation for both materials and production methods investigated in the BAM project.

The most important process parameters affecting the targeted properties of the final materials (including high mechanical strength, blast, impact and fire resistance, low density, thermal stability at elevated temperatures and structural integrity after exposure to fire), were assessed in laboratory scale. Among the investigated process parameters, those influencing the rheology of the geopolymer paste used for casting or 3D printing, were considered the most significant.

Both the new HLM and SCGC materials designed in the BAM project were successfully produced using both casting and 3D printing processes, with the exception of the 3D printing of UHPFRC, which was not feasible due to the large volume of steel fibers, despite significant efforts by the research team. Additionally, both new materials successfully met nearly all targeted properties to a high standard. The findings included in Deliverable **D4.2** will contribute to Deliverables **D4.3**, **D5.1**, and **D5.2** of the project.



## 2. Validation of the Impact- and Blast-resistant Material Performance

The work performed in WP3, Task 3.1, resulted in the optimization of the UHPFRC that was used as the impact/blast-resistant layer of the new Hybrid Laminated Material (HLM). Partner UCY coordinated the consortium efforts in a systematic and effective manner, by investigating the effects of different mix design parameters (e.g., water to binder (w/b) ratio, fibre content and type (steel only and steel and PVA combinations), steel fibre lengths, sand type, superplasticizer type and content, mixing speed and time, volume of mixture and method of fibre placement) to the mechanical strengths (compressive and flexural) of the final materials. This investigation yielded significant information regarding the abovementioned aspects. As an initial modification of the reference mixture, the possibility of substituting local sand with standard silica sand was explored. This change aimed to mitigate the significant delays and increased costs associated with sieving local sand to obtain the necessary quantities of fractions required for the development of the UHPFRC material. Various tests on mixtures containing different types, contents and denominations of fibres, and w/b ratios, showed that standard sand produced favorable results compared to the local sand, thus the standard silica sand use was adopted throughout the second phase of experimental development. During this phase, the consortium performed a series of designed optimization attempts to identify the minimum amount of fibres necessary to achieve the benchmark requirements set in the BAM project for the UHPFRC layer of the HML (150 MPa compressive and 20 MPa flexural strengths). After iterative mix development and properties' evaluation trials, the team successfully met the project's minimum compressive strength requirement of 150 MPa, with a mixture containing 2% steel fibres and 1% polyvinyl alcohol (PVA) fibres, and a low w/b ratio of 0.16. The mixture with 2% steel fibres (of 6mm and 12mm lengths at 1:1 ratio) and 1% PVA fibres demonstrated the highest flexural strength of 29.5 MPa, surpassing the required target of 20 MPa. The mix-design of the specific mixture is presented in Table 1.

**Table 1:** Optimized mixture of UHPFRC.

<i>Constituent</i>	<i>Steel Fibers 2% &amp; PVA 1%</i>
	<i>Content (kg/m<sup>3</sup>)</i>
Cement	880
Microsilica	220
Reference Sand	833
Water	172
Superplasticizer	67
Steel fibres 6mm	80
Steel fibres 13mm	80
PVA fibres	13
Water/Binder	0.16

In the last step of the UHPFRC development, the experimental work focused on the enhancement of workability, by increasing the water-to-binder (w/b) ratio to 0.21 (essentially increasing the water content to 231 kg/m<sup>3</sup>) and incorporating higher quantities of superplasticizer, making the mixture a self-compacting UHPFRC, improving its practicality. The self-compacting (SCC) version of the mix did not meet the minimum strength requirements set in BAM project. Therefore, the UHPFRC mix design with w/b ratio of 0.16 (Table 1) was further examined and used to cast the HLM.

An extended experimental work series has been conducted to determine the mechanical properties of the optimized mix. The average density, compressive, flexural, tensile strength, as well as Poisson's ratio and Modulus of Elasticity values obtained are presented in Table 2.

**Table 2:** Optimized UHPFRC Material Properties.

<b>Material Property</b>	<b>Value</b>	<b>Unit</b>
Density	2270	Kg/m <sup>3</sup>
Compressive Strength from cubes (100 mm × 100 mm × 100 mm)	154.55	MPa
Modulus of Elasticity from loading cylinders in compression	55.72	GPa
Poisson's Ratio	0.24	
Tensile Strength from dog-bone specimens	10.53	MPa
Cross-sectional area: (50 mm × 25mm)		
Modulus of Elasticity from direct tension test on dog-bone specimens	50.56	GPa
Tensile Strength from prisms	8.9	MPa
Cross-sectional area: (100 mm × 50 mm)		
Modulus of Elasticity from direct tension test on prisms	39.5	GPa
Flexural Strength from prismatic beams (100 mm × 100 mm × 500 mm) (3 point bending test)	29.47	MPa

Stress-strain relationships were obtained through experimental loading of cylindrical specimens in compression (Figure 1), direct tension tests on dog-bone specimens (Figure 2) and direct tension tests on prismatic specimens (Figure 3). The curves obtained are presented as follows.

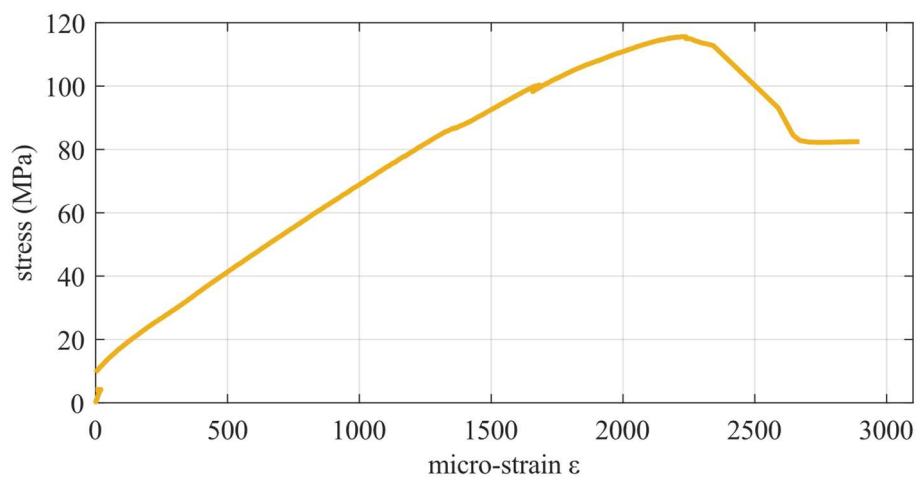


**Figure 1:** Stress-strain relationship from loading cylindrical specimens in compression.

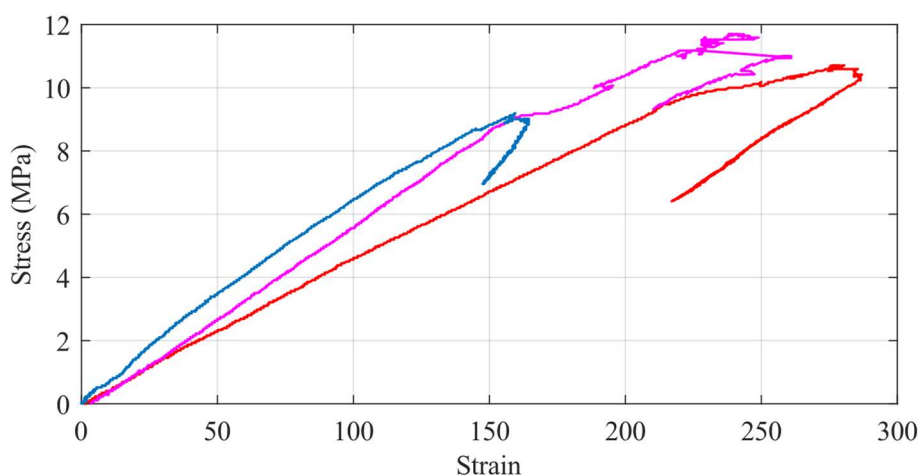


**Figure 2:** Stress-strain relationship from direct tension tests on dog-bone specimens.

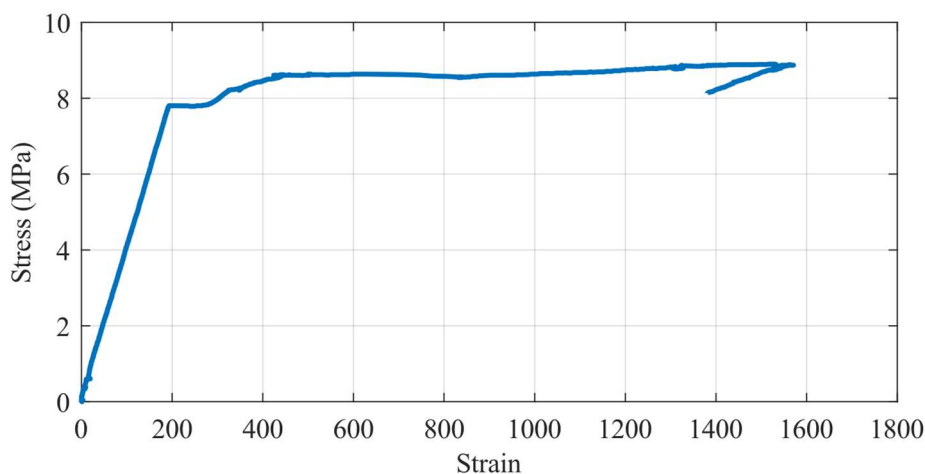


**Figure 3:** Stress-strain relationship from direct tension tests on prismatic specimens.

Furthermore, the following images present one of the dog-bone specimens (Figure 4a), tested in direct tension and one of the prismatic specimens (Figure 4 b), also tested in direct tension to determine tensile strength and Modulus of Elasticity of the optimized mixture.

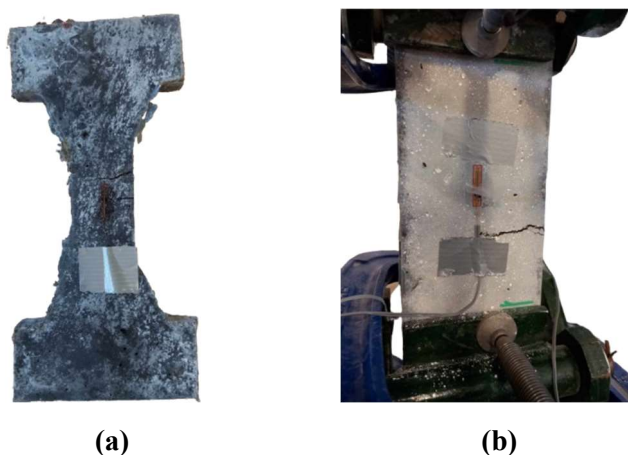


**Figure 4:** (a) Dog-bone specimen (cross-sectional area 50 x 25mm) and (b) Prismatic specimen (cross-sectional area 100 x 50 mm).

Presented below are the results of the preliminary drop-weight impact testing conducted at the National Centre for Scientific Research "Demokritos" (NCSR) in Athens, Greece. The aim of this preliminary investigation was to evaluate the material's performance under impact testing and, most importantly, to obtain the necessary performance parameters for the numerical modelling of the material's blast performance (Deliverable D4.3: Numerical Analysis of Blast Effect). Based on the experimental results and observations, it is evident that the specimens can absorb substantial amounts of drop-weight impact energy. This is due to the fibres in the material's matrix, which provide crack bridging and dissipate frictional energy when pulled from the matrix. The final report from NCSR is provided below:

24 May 2023

Dr. Demetris Nicolaides  
Frederick Research Center  
7 Yianni Frederickou Street,  
Pallouriotissa  
1036 Nicosia, Cyprus

### DROP-WEIGHT IMPACT OF DISK SPECIMENS

Disc-shaped specimens (grey ceramic with steel fibres) of the same material with dimensions  $\Phi 60 \times 10$  mm have been tested under drop-weight impact with various impact energy levels.

#### Methodological:

Four specimens were tested by dropping a weight of 670g from a height of 0.5m, 1.0m, 1.5m and 2m (impact energy of 3.3J, 6.6J, 9.9J and 13.2J respectively). The specimens after testing are shown in Figure 1.



**Figure 1. Under-surface of specimens after impact from heights of 0.5m, 1.0m, 1.5m and 2m (left to right). Appreciable deformation and multiple cracking is observed. Energy dissipation is evident by crack bridging and by the steel fibers.**

The testing frame, the drop weight and the specimen supporting ring used are shown in figure 2. The drop weight is made of brass and has a tip made of WC-Co with a flat tip of diameter 6mm. The weight is guided by the vertical tube and a load vs time graph is obtained by the use of a fast-response compression load sensor under a supporting ring of inner diameter 44mm. The load recording has a resolution of  $\pm 5$  N and an accuracy of  $\pm 10$  N. Time is recorded with a resolution of 1  $\mu$ s.

For the tests, the specimens were used as received. The ambient temperature was  $23 \pm 2^\circ\text{C}$  and the ambient relative humidity was  $50 \pm 5\%$ .



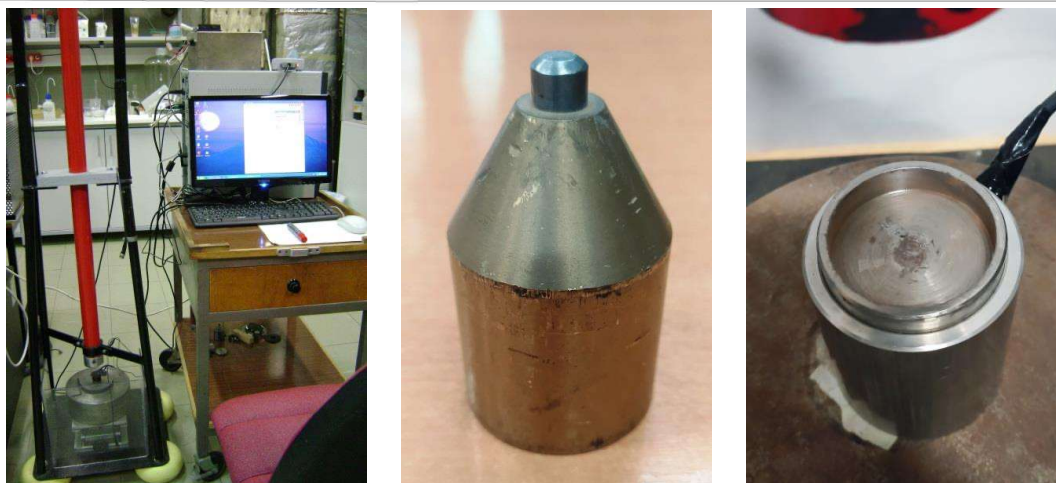


Figure 2. The drop-weight testing frame (left), the drop weight used (centre) and the ring support (right) used.

### Results:

From the raw signal-time curves, the load-deformation curves for the four tests (at different drop heights) were obtained and shown in figure 3. The main peak appears at about 0.5 – 1.3mm and reaches about 6000N for all specimens as expected. All the data are shown in the accompanying excel sheet.

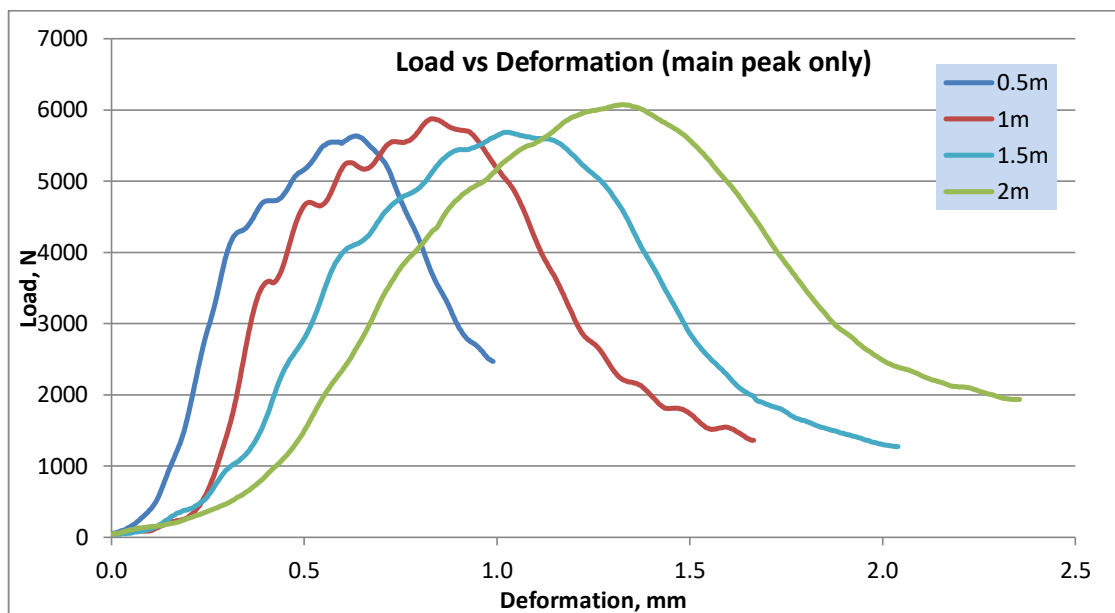
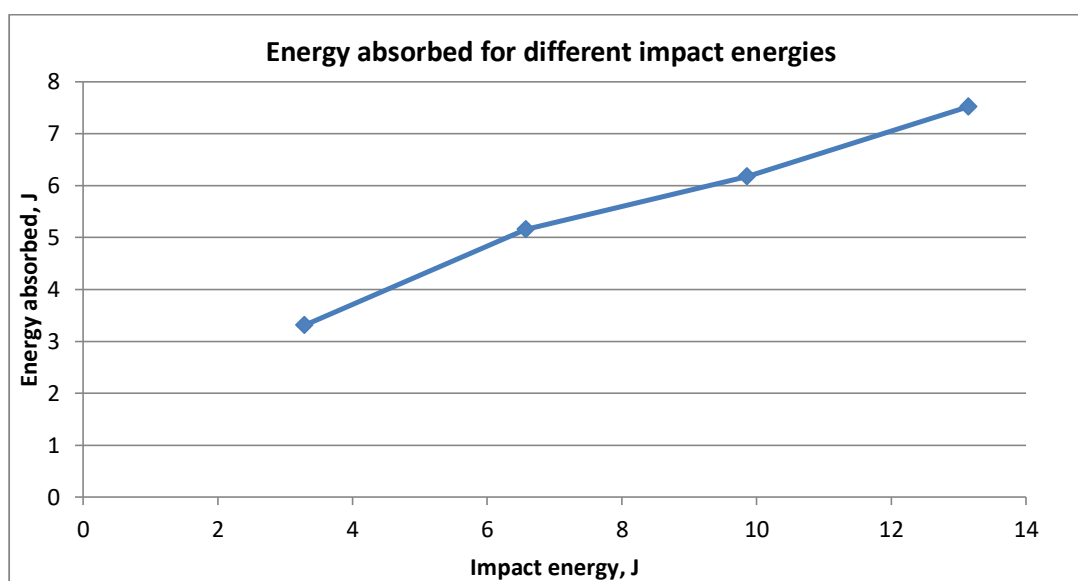


Figure 3. The load-deformation curves for the four tests.

The total energy absorbed by each specimen is given by the area under the main impact peak in figure 3 and the results are given in Table 1 and figure 4 (the raw curves also show a second peak due to the bounce of the weight which is not taken into account).

**Table 1. Summary of the results for energy absorption.**

Drop height	0.5m	1.0m	1.5m	2.0m
Impact energy, J	3.3	6.6	9.9	13.2
Energy absorbed (peak area), J	3.3	5.2	6.2	7.5
Ratio energy absorbed, %	100	78	63	57


**Figure 4. Energy absorbed by each specimen as a function of impact energy.**

The results indicate that the specimens are able to absorb substantial amounts of drop-weight impact energy, ranging from 100% for a drop height of 0.5m to 57% for a drop height of 2m. The energy absorbed appears to be an approximately linear function of the impact energy.

These results are in apparent agreement with the extent of the fractures of the specimens observed as shown in Figure 1. Whereas the lowest impact energy has only just initiated cracking in the specimen (leftmost in figure 1), increasing impact energy has resulted in increased fracturing. Energy absorption is apparently enabled by the steel fibres bridging the cracks and also by the fibres pulling out from the matrix due to frictional energy dissipation.

### 3. Validation of the Fire-Resistant Geopolymers Performance

#### 3.1 The Fire-Resistant Geopolymer (FRG) Layer of the HLM

In WP3, Task 3.1, a fire-resistant geopolymer (FRG) was designed, developed and optimized to be used as the fire protective layer of the new Hybrid Laminated Material (HLM). Partner FRC (Frederick Research Center) coordinated the efforts for the optimization of the FRG material, through systematic investigation of the basic geopolymerization process parameters (e.g., composition of the geopolymer binder, solid-to-liquid (S/L) ratio, type of the alkaline activator, addition of soluble silicates and molar ratio of silica to alkali-oxide in the activator). Deliverable “D3.1-Design and Development of Hybrid Laminated Material (HLM)” provides details on the development and optimization of the FRG material. The properties of the optimized FRG material were validated in the laboratory and Table 3 summarizes the results.

**Table 3:** Properties of the optimized FRG material.

Property of FRG	Value
Density (g/cm <sup>3</sup> )	1.48
Compressive strength (MPa)	25.39
Residual compressive strength after exposure to 600 °C (MPa)	41.39
Density after exposure to 600 °C (g/cm <sup>3</sup> )	1.43
Mass loss after exposure to 600 °C (%)	7.00
Linear shrinkage after exposure to 600 °C (%)	1.20
Residual compressive strength after exposure to 800 °C (MPa)	38.64
Density after exposure to 800 °C (g/cm <sup>3</sup> )	1.37
Mass loss after exposure to 800 °C (%)	8.40
Linear shrinkage after exposure to 800 °C (%)	1.10
Residual compressive strength after exposure to 1050 °C (MPa)	27.18
Density after exposure to 1050 °C (g/cm <sup>3</sup> )	1.38
Mass loss after exposure to 1050 °C (%)	9.30
Linear shrinkage after exposure to 1050 °C (%)	1.50

The performance of the optimal FRG material against fire was assessed according to the standard ISO 834 time-temperature curve (Fire-resistance tests – Elements of building constructions)<sup>[1]</sup>. The specimens used for this fire testing were of dimensions 12x12x24 cm<sup>3</sup>, consisting an FRG board and a concrete slab of 20 cm thickness prepared according to the EFNARC specifications<sup>[2]</sup>.

<sup>[1]</sup> ISO, 834: *Fire Resistance Tests – Elements of Buildings Construction*, International Organization for Standardization, Geneva, 1999

<sup>[2]</sup> EFNARC, European Federation of National Associations Representing producers and applicators of specialist building products for Concrete: Specification and guidelines for testing of passive fire protection for concrete Tunnels lining, 2009



The board of FRG material was fastened on the concrete slab with fire-resistant stainless-steel anchors (Fischer FNA 6x30/30 A4).

The fire resistance test was performed in a custom-made furnace working with electric resistors (Carbolite RHF1600). The furnace had the ability to simulate all the standard time – temperature curves beginning from ISO 834, which reaches a maximum temperature of 1050 °C. The tested specimen was installed tightly onto the opening of the furnace so as its front surface (front side) to be exposed at a heat flux during the whole test, simulating the ISO 834 time-temperature curve scenario. The furnace was rapidly heated at a rate of up to 100 °C/min, using specific silicon carbide (SiC) heating elements. Fire resistance test was carried out over 90 minutes and the temperatures at the specimen's surface located on furnace opening (front side) at a distance of about 22 cm from this surface (middle distance) and at the interface of the specimen with the concrete slab (back side of specimen) were recorded using thermocouples of K-type (NiCr-Ni). The temperature inside the furnace was continuously recorded, using two thermocouples placed at the furnace center. The heating rate of ISO 384 standard time-temperature curve is defined by Equation (1).

$$T = T_0 + 345 \times \log_{10} (8 \times t + 1) \quad (1)$$

where,  $T$ : furnace temperature (°C) at  $t$ ,  $T_0$ : initial furnace temperature (°C) and  $t$ : elapsed time (min).

This (theoretical) ISO 834 fire-curve is shown in Figure 5, along with the actual heating curve obtained on the refractory brick using the furnace<sup>[3]</sup> over 90 minutes.

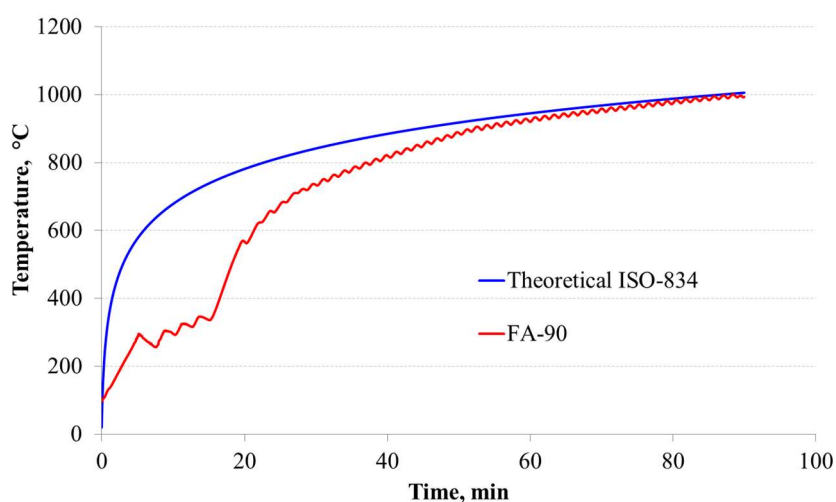


**Figure 5:** Furnace temperature profile during the FRG material fire test (standard ISO 834 fire curve).

<sup>3</sup> ISO 834 assumes the use of a pre-heated gas-fired furnace whereas the test presented in this report was carried out using an electrical furnace.

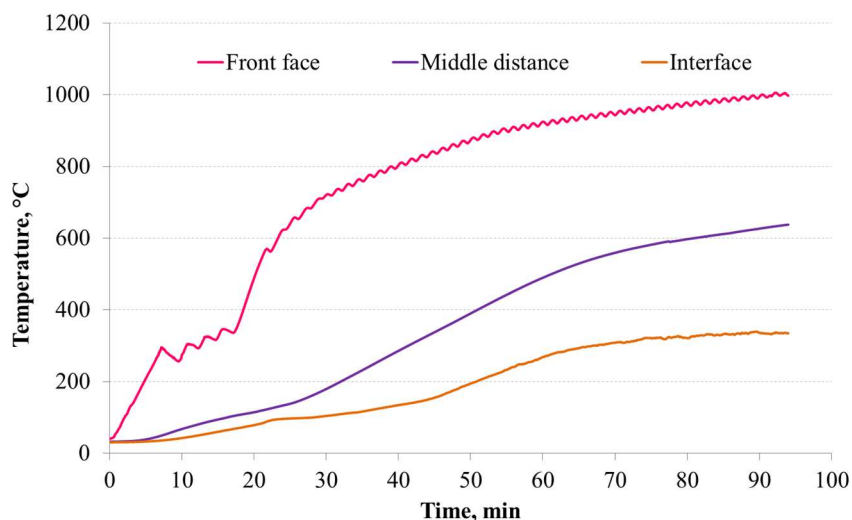


**Figure 6:** Temperature profile on the FRG specimen's front side, at a distance of 22 cm from the front side and at the interface of concrete slab.

According to Figure 6, the tested FRG material succeeded under the ISO 834 curve based on the requirements (limits) of the specific standard for approximately 60 minutes, without undergoing any damage, yielding or spalling phenomena. The tested specimen of the FRG material before and after the fire test is shown in Figure 7.

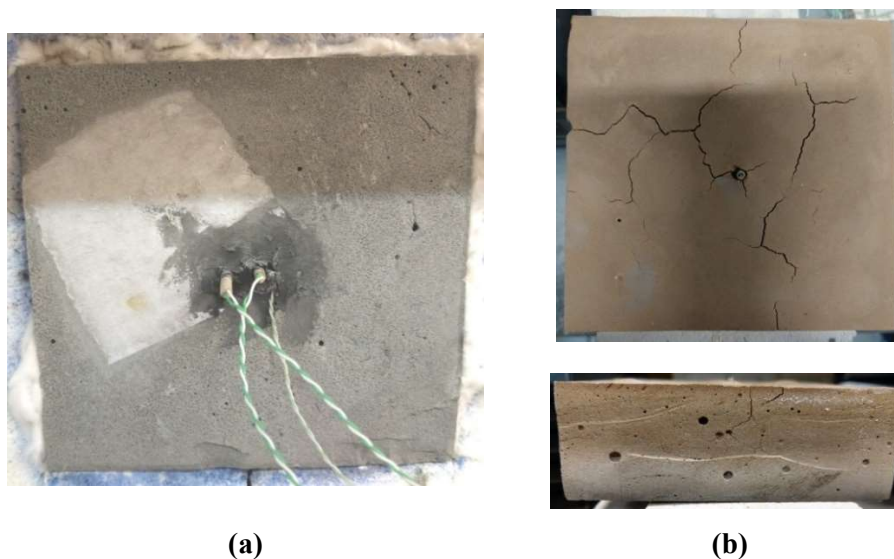


**Figure 7:** The FRG specimen (a) before and (b) after the standard ISO 834 fire test.

As it is shown in Figure 7, only very limited surface micro-cracking appeared on the FRG specimen after 90 minutes of exposure to fire, according to the ISO 834 fire-curve. The concrete slab protected by the fire-resistant material did not appear any form of spalling or other mechanical damage and remained as it was initially before the fire test, thus indicating the success and suitability of the developed FRG material as a fire-resistant protective layer.

### 3.2 The Smart Composite Geopolymeric Concrete (SCGC)

In WP3, Task 3.2, a smart composite geopolymeric concrete (SCGC) aimed at providing buildings and constructions with combined fire-, blast- and impact-resistance was designed, developed and optimized. Partner FRC (Frederick Research Center) coordinated the efforts for the development and optimization of the SCGC, through a systematic investigation of important geopolymerization process parameters (e.g., solid-to-liquid (S/L) ratio, volumetric ratio of silicate and hydroxide solutions in the alkaline activator, addition of solid materials to improve the mechanical strength, type and content of fibers addition). Details about the development and optimization of the SCGC material are given in Deliverable “D3.2-Smart Composite Geopolymeric Concrete (SCGC). In Table 4 below, the main properties of the optimized SCGC material are summarized.

**Table 4:** Properties of the optimized SCGC material.

Property of SCGC	Value
Density (g/cm <sup>3</sup> )	2.12
Compressive strength (MPa)	135.47
Flexural strength (MPa)	8.60
Water absorption (% wt.)	< 0.05

The performance of the optimized SCGC material against fire was assessed based on the standard ISO 834 time-temperature curve. Details on the fire test requirements and the followed procedure are described in Section 3.1 above, of this Deliverable. The temperature profile of the furnace and the surfaces of the SCGC specimen exposed to fire are shown in Figures 8 and 9 below.

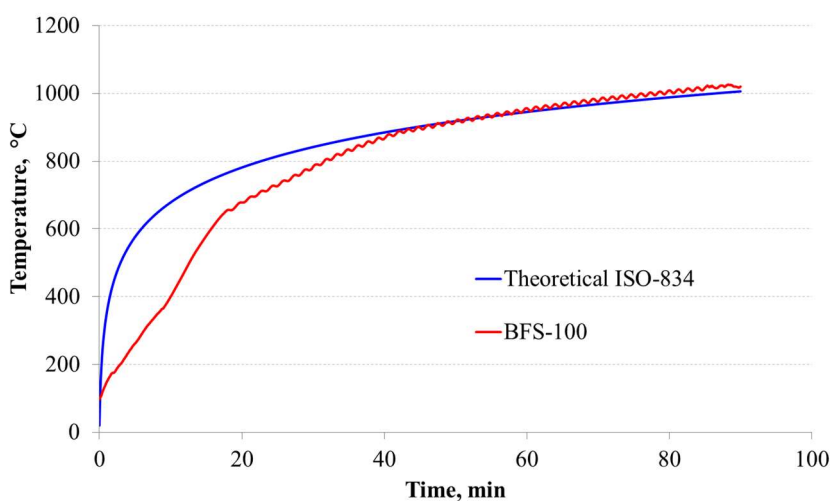


**Figure 8:** Furnace temperature profile during the SCGC fire test (standard ISO 834 fire curve).

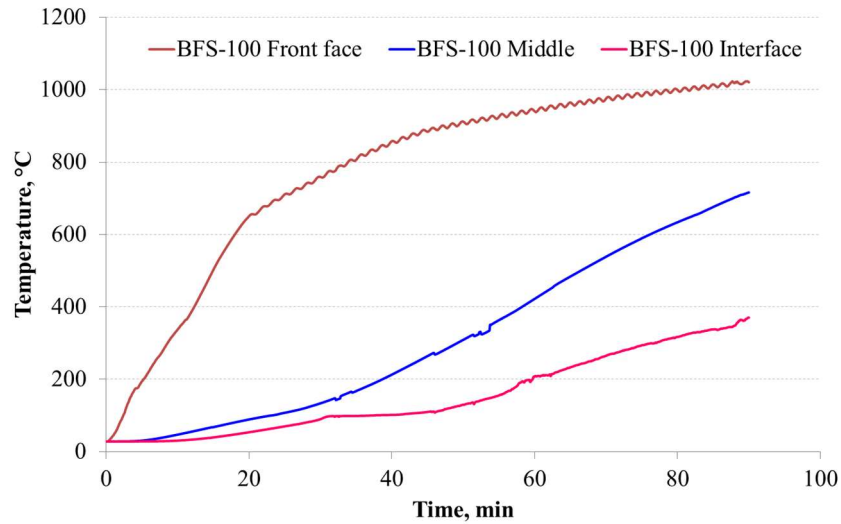


**Figure 9:** Temperature profile on the SCGC specimen's front side, at a distance of about 20 cm from the front side and at the interface of SCGC with the concrete slab.

According to Figure 9, the tested SCGC material succeeded under the ISO curve based on the requirements (limits) of the specific standard for a period of about 60 min, without presenting spalling phenomena or undergoing any damage or collapse. It is important to note that prior to the fire testing, the SCGC specimen presented a widespread cracking on its back side (Figure 10a), while after the test extended cracking also appeared at the front side of the specimen, the one that was exposed to fire (Figure 10b).

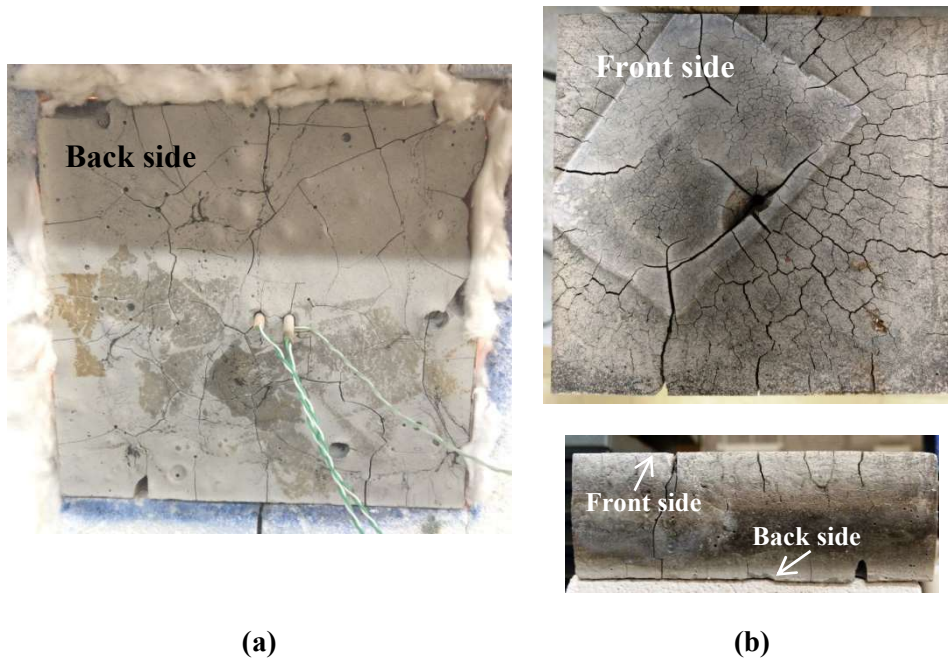


**Figure 10:** The FRG specimen (a) before and (b) after the standard ISO 834 fire test.

The extended cracking that occurred on both surfaces of the SCGC specimen (Figure 10) after the fire test is probably the reason for the material's failure to withstand the standard ISO 834 time-temperature curve for a period extending 60 minutes. However, the concrete slab protected by the SCGS fire-resistant material did not appear any spalling or other mechanical damage and remained as it was initially before the fire test. Therefore, it can be safely concluded that the SCGC can also protect a concrete structure against fire for a considerable period of time, even if it loses its mechanical cohesion and needs to be replaced after the fire.

## 4. Comparative Analysis of Fire Resistance in Standard Concrete and the New Materials HLM and SCGC

This study aims to assess and compare the fire resistance of three different systems based on standard concrete and the two materials developed in BAM project, the HLM and the SCGC. This comparative study aims to offer insights about their effectiveness against fire. Additionally, the investigation will evaluate the overall performance of the new materials for the protection of buildings and structures against fire. These insights will contribute to their validation in terms of both fire resistance and adhesion bond, thus enhancing their reliability in practical applications. The comparison process begins with the preparation of three specimens, including three cubes: a standard concrete cube with consistent dimensions and strength used as a reference, and two others, each consisting of a layer of the relevant BAM material developed in WP3, either HLM (Task 3.1) or SCGC (Task 3.2), applied to a standard concrete cube for adhesion purposes. Subsequently, the three prepared cubes undergo controlled fire exposure testing. This involves subjecting them to specified temperatures and durations of fire exposure, while monitoring and recording data regarding the temperature inside the concrete cubes (near the interface of the new material and the concrete cube, as well as at the back side of the concrete cube), duration of exposure, and any observed physical alterations. Evaluating the adhesion quality of HLM and SCGC materials as protective layers for buildings and structures is essential to ensure secure attachment to the concrete cubes, particularly considering the potential detachment caused by the rapid increase in temperature at the contact adhesion points during a fire.

### 4.1 Materials and methods

The materials utilized in this experimental procedure comprise of a standard concrete cube, designated as the reference sample, featuring dimensions of 15.0x15.0x15.0 cm and compressive strength of 60.0 MPa. The mix design composition per 1 m<sup>3</sup> is presented in Table 5.

**Table 5.** Mix design composition for standard concrete cubes (1 m<sup>3</sup>).

Materials	Quantity (kg or L)
Portland Cement 42.5	475
Diabase Aggregates 8/20 mm	657
Diabase Aggregates 4/10 mm	357
Diabase Sand 0/4 mm	320
Limestone Sand 0/2 mm	481
Superplasticizer (L)	3.8
Retarder (L)	1.9
Water (L)	157



The fire-resistant geopolymer (FRG) layer, a component of the Hybrid Laminate Material (HLM), measures 15.0x15.0x3.0 cm and is affixed to the surface of the second concrete cube, to assemble the second system (HGFRL-CC), as illustrated in Figure 11 – [A]. The mix design composition is presented in Table 6 below.

**Table 6.** Mix design composition of hybrid laminate fire resistant geopolymer (900 cm<sup>3</sup>).

Materials	Quantity (g or mL)
Fly Ash-90 (g)	450
GGBFS-10 (g)	50
[7M] NaOH (SH) (mL)	41
Na <sub>2</sub> SiO <sub>3</sub> .xH <sub>2</sub> O (SS) (mL)	91
Ratios	
S/L (kg/L)	3.80
SH/SS (v/v)	0.45

Similarly, in the third system (SCGL-CC), the smart composite geopolymeric concrete layer, also of dimensions 15.0x15.0x3.0 cm, is attached to another concrete cube (Figure 11 – [B]). The mix design composition of the SCGC is presented in Table 7 below.

**Table 7.** Mix design composition of smart composite geopolymer concrete (900 cm<sup>3</sup>).

Materials	Quantity (g or mL)
GGBFS-10	800
[7M] NaOH (SH) mL	100
Na <sub>2</sub> SiO <sub>3</sub> .xH <sub>2</sub> O (SS) mL	150
Ratios	
S/L (kg/L)	3.20
SH/SS	0.67

It is essential to emphasize that across all the three configurations, the concrete cubes possess identical characteristics, ensuring consistency and reliability in the evaluation of the fire performance.

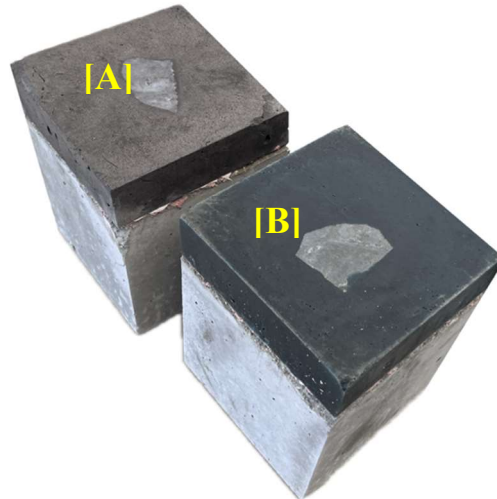


**Figure 11:** Attachment of geopolymer layers to concrete cubes in HGFR-L-CB [A] and SCGL-CB [B] systems.

The attachment process for the second and third concrete systems involved first the application of quartz adhesion primer, followed by high-temperature sealant silicone on both surfaces. Figure 2 illustrates the adhesion bond procedure, especially the methodology and the materials utilized for the attachment of the Smart Composite Geopolymeric Concrete onto the standard concrete cube.



**Figure 12:** Application of quartz adhesion primer [a] and sealant silicone [b] on the Surfaces of smart composite geopolymeric concrete and concrete cube.



## 4.2 Fire Exposure Testing

The three distinct systems underwent exposure to fire utilizing a blow torch as the primary heat source. For reference, the systems are denoted as "SCC" "HGFRL-CC" and "SCGM-CC", respectively. Thermocouples were strategically placed at specific locations inside the cubes through pre-drilled holes, to monitor temperature variations within the concrete cubes during fire exposure. For the SCC sample, thermocouples were positioned at "SCC- A" (1) and "SCC-B" (2). In the combined systems, thermocouples "HGFRL-CC- A" (3), "HGFRL-CC-B" (4), "SCGM-CC- A" (5), and "SCGL-CC-B" (6) were utilized. Checkpoints A and B were chosen to measure temperatures at two specific locations: 8 cm from the exposed surface and 2 cm from the rear surface. The positioning of each thermocouple is illustrated in Figure 13.

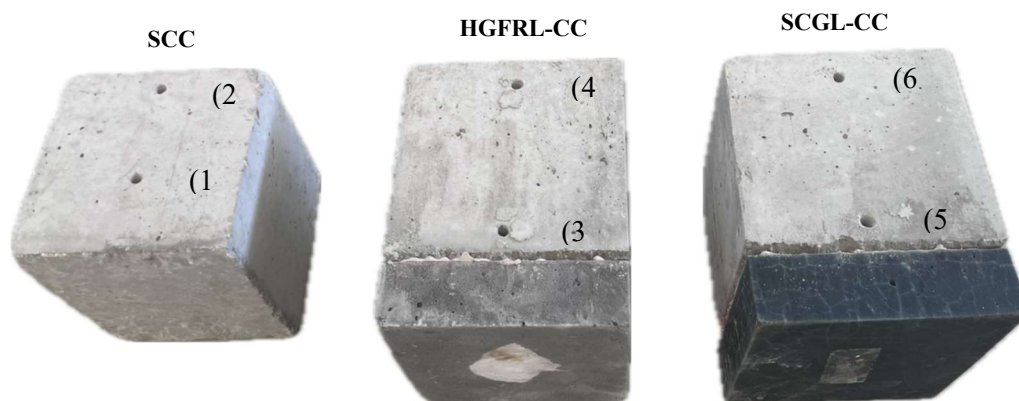


**Figure 13:** Positioning of thermocouples in SCC, HGFRL-CC, and SCGM-CC systems during fire exposure.

The six (6) thermocouples were essential for measuring and monitoring the temperature fluctuations inside the concrete cubes due to the heat transfer during the fire exposure. The fire testing setup is shown in Figure 14 below.



**Figure 14:** Fire testing setup illustrating the placement of six thermocouples for monitoring temperature fluctuations inside concrete cubes.

The thermocouples utilized were DS18B20 sensors, known for their high accuracy and reliability. These sensors have a temperature measurement range between  $-55^{\circ}\text{C}$  to  $+125^{\circ}\text{C}$  and provide precise temperature readings with a typical response time of under 750 ms at 12-bit resolution and an accuracy of  $\pm 0.5^{\circ}\text{C}$  within the range of  $-10^{\circ}\text{C}$  to  $+85^{\circ}\text{C}$ . The sensors were programmed on an ESP32 board, which was connected to a PC for recording temperature data every 5 minutes over a total fire testing duration of 100 minutes (Figure 15).

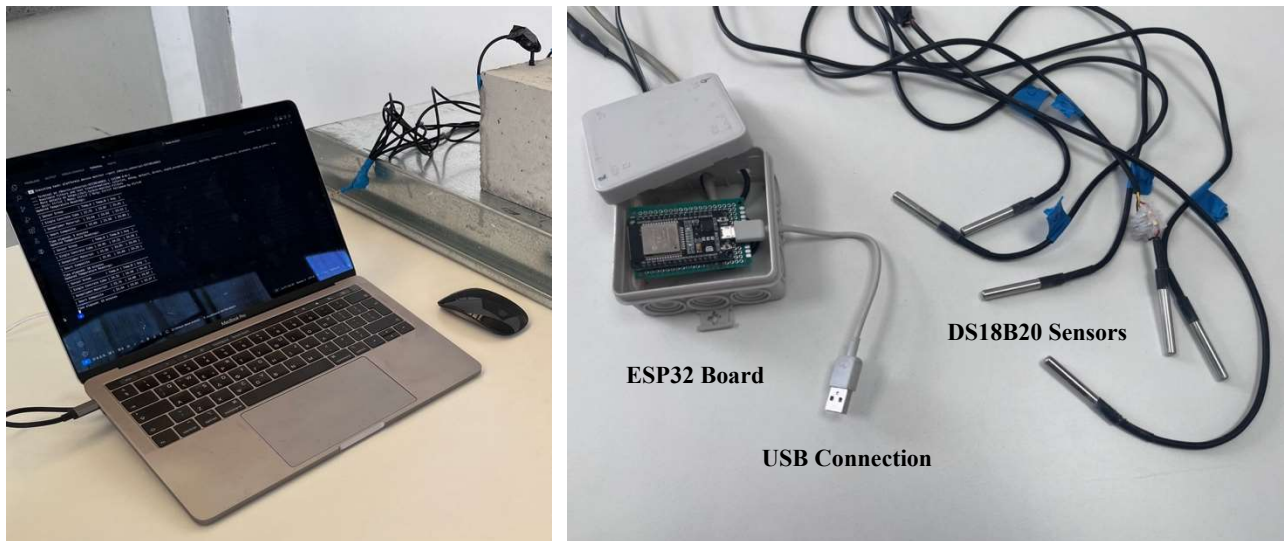


**Figure 15:** PC interface connected to ESP32 board for recording temperature data from DS18B20 sensors.

### 4.3 Data Collection

The data collection process involved the use of six thermocouples strategically positioned, as previously presented in Figure 13, to monitor temperature changes during the specimens' fire exposure. These thermocouples provided real-time temperature data, which were recorded continuously throughout the experiment and stored locally on a PC for subsequent analysis.

Data collected from the thermocouples were organized and presented in Table 8 below for clear comparisons between the different systems, highlighting the effectiveness of the fire-resistant (FRG) and smart composite geopolymer (SCGC) layers in enhancing the thermal performance of the concrete cubes.

The collected data provided valuable insights into the heat transfer dynamics and aided in evaluating the effectiveness of the different systems in terms of fire resistance. Observations regarding the physical and structural changes in the systems during and after fire exposure, as well as any detachment or degradation of the geopolymer layers, are discussed in the following section on data analysis.

**Table 8.** Temperature data collected from thermocouples for standard concrete cube, hybrid geopolymer fire resistant layer, and smart composite geopolymer material during fire exposure.

Time (min)	Standard Concrete Cube Checkpoints		Hybrid Laminate Fire Resistant Geopolymer Checkpoints		Smart Composite Geopolymer Concrete Checkpoints	
	SCC-A (1) (°C)	SCC-B (2) (°C)	HGFRL-CC-A (3) (°C)	HGFRL-CC-B (4) (°C)	SCGL-CC-A (5) (°C)	SCGL-CC-B (6) (°C)
0	35.75	36.19	35.63	36.06	36.38	36.19
5	35.75	36.31	35.81	36.19	36.44	36.31
10	39.25	36.38	35.94	36.25	36.63	36.38
15	47.75	36.50	37.00	36.31	37.35	36.41
20	57.75	36.63	39.00	36.44	38.94	36.50
25	66.75	37.00	41.63	36.50	41.37	36.58
30	75.25	37.50	44.31	36.63	43.88	36.69
35	82.25	38.25	47.00	36.69	46.81	36.75
40	88.25	39.19	49.69	36.81	49.88	36.81
45	92.50	40.31	52.25	36.94	53.23	36.97
50	95.50	41.50	54.69	37.06	56.00	37.06
55	97.25	42.81	56.94	37.19	58.94	37.19
60	98.25	44.25	58.94	37.38	60.86	37.45
65	99.00	45.50	60.78	37.82	63.15	37.89
70	99.70	47.00	62.53	38.26	64.31	38.33
75	100.50	48.50	64.15	38.82	66.19	38.89
80	101.20	50.19	65.65	39.88	68.06	39.95
85	102.00	51.63	67.72	41.42	69.94	41.63
90	102.70	52.94	69.78	42.93	71.50	43.13
95	103.50	54.38	70.28	44.31	72.75	44.68
100	104.30	55.69	71.98	45.90	73.56	46.00

#### 4.4 Data Visualization

To facilitate a comprehensive analysis of the thermal performance of the systems under fire exposure, the recorded temperature data has been graphically represented. The graph in Figure 16 depicts the temperature variations over time for each of the configurations tested. This visualization enables a clear comparison of the thermal behavior and efficiency of the different protective layers in mitigating heat transfer. The graph highlights critical trends reached during

the experiment, offering valuable insights into the efficacy of the geopolymer layers in enhancing fire resistance.

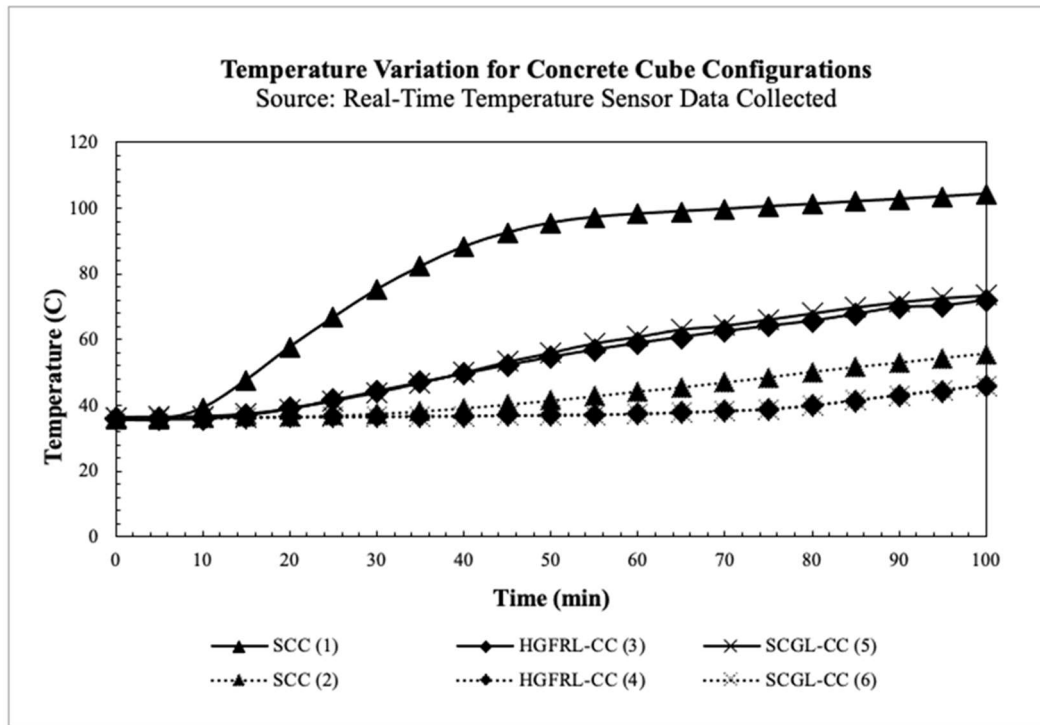


**Figure 16:** Temperature variation over time for different concrete cubes configurations.

## 4.5 Data Analysis

The following data analysis delves into the thermal performance of three distinct concrete cube systems during fire exposure: a standard concrete cube (SCC), a concrete cube shielded with a fire-resistant geopolymer layer (HGFR-CC), and a concrete cube shielded with a smart composite geopolymer layer (SCGL-CC). Parameters such as percentage difference in temperature, maximum temperature reached, temperature gradient, rate of temperature increase, thermal stability, physical and structural integrity, and adhesion quality of the protective layers will be examined in detail to draw comprehensive conclusions about the performance of each system.

### 1. Percentage Difference in Temperature

The percentage difference in temperature between various systems serves as an important parameter for evaluating thermal performance, effectiveness of protective measures and safety, particularly in fire exposure scenarios. This metric allows for comparative assessment of how effectively different systems mitigate temperature rise or maintain lower temperatures compared to reference materials. It provides valuable insight into thermal behavior, aiding in the

optimization of design for improved heat dissipation and insulation. This parameter can be calculated using the following formula:

$$\text{Percentage difference} = \frac{\text{Temperature of System} - \text{Reference Temperature (SCC)}}{\text{Reference Temperature (SCC)}} \times 100$$

The table below shows the percentage difference at the final time point (100 minutes):

System	Checkpoint A (%)	Checkpoint B (%)
SCC (Standard Concrete Cube)	0%	0%
HGFRL-CC (Fire-Resistant Layer)	-30.98%	-17.63%
SCGL-CC (Smart Composite Layer)	-29.47%	-17.38%

## 2. Maximum Temperature Reached

The maximum temperature reached during the fire exposure test is a critical parameter for evaluating the fire resistance and thermal performance of the different concrete cube configurations. This measure provides insight into the peak thermal load that each configuration can withstand before undergoing significant structural or material changes. By comparing the maximum temperatures recorded by thermocouples in the standard concrete cube (SCC), the concrete cube with the fire-resistant geopolymer layer (HGFRL-CC), and the concrete cube with the smart composite geopolymer layer (SCGL-CC), we can assess the effectiveness of these protective layers in enhancing the fire resistance of the concrete. Higher maximum temperatures in the standard concrete cube, compared to those with protective layers, indicate the additional thermal insulation provided by the geopolymer layers, thus demonstrating their potential in improving fire resistance in construction applications.

The maximum temperatures reached at each checkpoint during the 100-minute test are as follows:

System	Checkpoint A (°C)	Checkpoint B (°C)
SCC (Standard Concrete Cube)	104.30	55.69
HGFRL-CC (Fire-Resistant Layer)	71.98	45.90
SCGL-CC (Smart Composite Layer)	73.56	46.00

## 3. Temperature Gradient

The temperature gradient within each concrete cube configuration during fire exposure provides crucial information on the heat transfer characteristics and the effectiveness of thermal protection and further insulation. This parameter is derived from the temperature difference between various points within the concrete cubes, particularly between the surface exposed to fire and internal



points. By analyzing the temperature gradient, we can evaluate how well the protective layers mitigate heat penetration into the concrete. A lower temperature gradient in concrete cubes with the fire-resistant geopolymer layer (HGFRL-CC) and the smart composite geopolymer layer (SCGL-CC) compared to the standard concrete cube (SCC) indicates superior thermal insulation properties, thereby enhancing the overall fire resistance.

The temperature gradient is the difference between Checkpoint A and Checkpoint B:

System	Temperature Gradient (°C)
SCC (Standard Concrete Cube)	48.61
HGFRL-CC (Fire-Resistant Layer )	26.08
SCGL-CC (Smart Composite Layer)	27.56

#### 4. Rate of Temperature Increase

The rate of temperature increase within each concrete cube configuration during fire exposure is a critical parameter for understanding how quickly heat is absorbed and transmitted through the material. This rate is calculated by measuring the temperature change over specific time intervals. A slower rate of temperature increase indicates that the material is effectively insulating and delaying the heat transfer, which is particularly important for enhancing fire resistance.

By comparing the rate of temperature increase among the standard concrete cube (SCC), the concrete cube with the fire-resistant geopolymer layer (HGFRL-CC), and the cube with the smart composite geopolymer layer (SCGL-CC), we can assess the efficacy of these protective layers. A significantly slower rate of increase in the HGFRL-CC and SCGL-CC configurations compared to the SCB suggests that these layers are providing additional thermal protection, making the material more resistant to fire.

The rate of temperature increase can be calculated by the slope of the temperature vs. time graph. A simple approximation is:

$$\text{Rate} = \frac{\text{Temperature at 100 minutes} - \text{Temperature at 0 minutes}}{100 \text{ minutes}}$$

System	Checkpoint A (°C/min)	Checkpoint B (°C/min)
SCC (Standard Concrete Cube)	0.686	0.195
HGFRL-CC (Fire-Resistant Layer)	0.362	0.099
SCGL-CC (Smart Composite Layer)	0.372	0.098

## 5. Thermal Stability

The thermal stability of each system can be inferred from the temperature fluctuations. Lower fluctuations indicate higher stability. Both HGFRL-CC and SCGL-CC systems showed minimal fluctuations compared to the SCC system, indicating higher stability.

## 6. Physical and Structural Integrity

Observations during the test indicated that the standard concrete cube (SCC) exhibited significant cracking and spalling, while both HGFRL-CC and SCGL-CC maintained better structural integrity with minimal surface degradation.

## 7. Adhesion Quality of Protective Layers

No significant detachment of the geopolymer layers was observed during the test, indicating good adhesion quality for both HGFRL-CC and SCGL-CC.

## 8. Visual Examination of Exposed Surfaces of Concrete Cube Systems

The following figures (Figure 17) provide a visual examination of the exposed surfaces of the three concrete cube systems after fire testing. These images illustrate the physical and structural changes that occurred due to heat exposure, offering additional insights into the fire resistance properties of each system. Notably, all systems exhibited cracks on the exposed surface, particularly on the smart composite geopolymer layer. However, despite these surface cracks, the heat transfer was not significantly affected, as evidenced by the temperature data and parameters analyzed above.

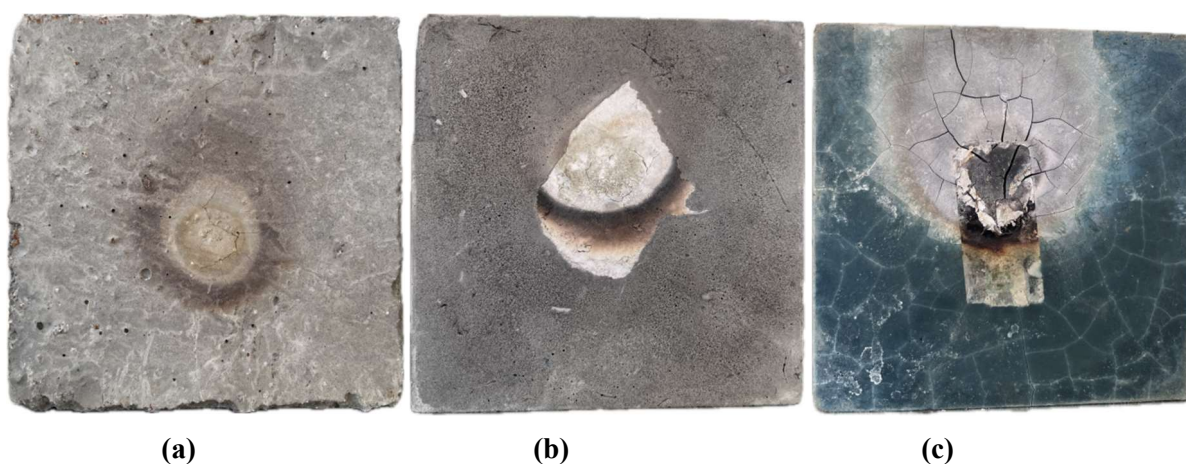


**Figure 17:** Exposed surface of (a) standard concrete cube (SCC) after fire testing; (b) of concrete cube with fire-resistant geopolymer layer (HGFRL-CC) after fire testing and (c) of concrete block with smart composite geopolymer layer (SCGL-CC) after fire testing.

## 9. Comparative Analysis

- SCC without any protective layers reached the highest temperatures at both Checkpoint A (104.3°C) and Checkpoint B (55.69°C). The rapid rate of temperature increase, and significant temperature gradient indicate inadequate thermal insulation.
- HGFRL-CC significantly reduced the temperature rise, with the maximum temperature at Checkpoint A being 71.98°C. The temperature gradient was also lower, indicating better heat distribution and insulation.
- SCGL-CC performed similarly to the fire-resistant layer, with a maximum temperature at Checkpoint A of 73.56°C. The temperature gradient and rate of increase were slightly higher than HGFRL-CC but still significantly lower than SCC.



## 5. Conclusions

- The targeted properties for the final materials developed in the BAM project were validated in a laboratory scale.
- The optimized UHPFRC layer of the HLM was validated with a composition of 2% steel fibers and 1% PVA fibers, along with the replacement of local sand with standard silica sand. These materials were chosen as the most cost-effective options that met the project's minimum strength requirements. Additionally, a self-compacting version of the 2% steel and 1% PVA UHPFRC was developed, which exhibited a 16.51% decrease in compressive strength and an 18.43% decrease in flexural strength.
- When no PVA fibres were included, the 2% steel fibre UHPFRC layer did not reach the project's strength requirements. The self-compacting version of this particular mix did not exhibit significant disparity in terms of strength, compared to its non-self-compacting equivalent.
- The rheological characteristics of the geopolymer paste and especially viscosity and setting time were proved of great significance for both the production processes investigated (i.e., casting and 3D printing). The most important geopolymerization process parameters affecting the viscosity and setting time of the geopolymeric paste were the ratio of the solid precursor to the liquid activator (S/L), the concentration of the alkali hydroxide solution, the volume ratio of the alkali hydroxide to the alkali silicate solutions in the activator, as well as the molar ratios Si/Al and Si/Alkali, in both cases of the production processes investigated.
- The compressive, flexural and tensile strengths, as well as the modulus of elasticity and the Poisson's ratio were considered as significant parameters for the UHPFRC material to achieve the desired impact resistance.
- The apparent density, compressive strength and thermal stability at elevated temperatures were considered as the most significant parameters for the fire-resistant geopolymers.
- The fire performance assessment of a standard concrete cube (SCC), a concrete cube with a fire-resistant geopolymer layer (HGFRL-CC), and a concrete cube with a smart composite geopolymer layer (SCGL-CC) revealed significant improvements in the thermal performance of the systems shielded with the developed fire-resistant materials. The SCC showed the highest rate of temperature increase, reaching over 100°C within 100 minutes of fire exposure. In contrast, the HGFRL-CC and SCGL-CC cubes demonstrated superior fire resistance, with lower temperature rates and better thermal insulation properties.

- The critical temperature threshold for concrete, known to cause potential structural damage, was reached more quickly in the standard concrete cube than in the cubes with protective layers. This underscores the importance of incorporating fire-resistant materials into construction to delay the onset of critical temperatures and mitigate damage.
- Furthermore, the smart composite geopolymer layer (SCGL-CC) exhibited the most effective fire resistance, maintaining the lowest temperatures throughout the testing period. This suggests that smart composite geopolymer layers could be highly beneficial in applications requiring enhanced fire and explosion resistance.
- In conclusion, the use of geopolymer materials as protective layers on new or existing concrete buildings and structures can improve their fire performance. The findings support the potential of these materials in enhancing structural safety and durability in fire-prone environments.
- Finally, the various versions of the developed UHPFRC materials (i.e., 2% steel + 1% PVA fibers, 6% steel fibers by volume) exhibited excellent performance against impact loads, making them a promising and reliable protective material against blast and impact loading.

## Acknowledgements

*The project is implemented under the programme of social cohesion “THALIA 2021-2027” co-funded by the European Union, through Research and Innovation Foundation.*

*Το έργο υλοποιείται στο πλαίσιο του Προγράμματος Πολιτικής Συνοχής «ΘΑΛΕΙΑ 2021-2027» με τη συγχρηματοδότηση της ΕΕ, μέσω του Ιδρύματος Έρευνας και Καινοτομίας.*

